2015-06-01

Characterization of Order-Disorder Phase Transition Temperature for Select Nanoparticles

Gregory J. Sutherland
Brigham Young University - Provo

Characterization of Order-Disorder Phase Transition Temperature for Select Nanoparticles

Gregory J. Sutherland

A thesis submitted to the faculty of
Brigham Young University
in partial fulfillment of the requirements for the degree of

Master of Science

Richard Vanfleet, Chair
Gus Hart
David Allred

Department of Physics and Astronomy

Brigham Young University

June 2015

ABSTRACT

Characterization of Order-Disorder Phase Transition
Temperature for Select Nanoparticles

Gregory J. Sutherland
Department of Physics and Astronomy, BYU
Master of Science

A method was found for creating ordered nanoparticles whose size and theoretical order-disorder temperature are ideal for study in the TEM. Specifically FePt, NiPt, FeNiPt and AuCu nanoparticles were studied. We were able to show how a nanoparticle's size affects its order-disorder temperature (Tod). When the particles were around 6 nm in diameter there was a shift downward of the Tod of 10-15 percent compared to the bulk. While particles around 10 nm in diameter experienced a downward shift of 0-6 percent compared to the bulk. One can approximate that particles less than 10-15 nm in diameter would show significant decreases in order-disorder temperature. We confirmed that alumina prevents copper losses, compositions were well within percent error. In addition we showed that when the alumina used is thin enough the images are not adversely affected and charging is not an issue.

Keywords: nanoparticle, order-disorder, FeNiPt, alumina

ACKNOWLEDGEMENTS

Thank you, Dr. Vanfleet, for your tutelage and example. Thank you for all your help and advice both in research and career.

Thank you, Dr. Allred, for your help with the alumina coating, your suggestions on our AuCu composition problems, and your encouragement.

Thank you, Dr. Hart, for bringing a computationalist's point of view to the table on this project.

Thanks to my family for always being there for me and encouraging me.

This work was supported by funding from the National Science Foundation (NSF) Division of Materials Research (DMR). Grant Number 0906385.

TABLE OF CONTENTS

LIST OF FIGURES

Chapter 1

Introduction

Our current advances in technology have been a direct result of our understanding of materials properties and our ability to manipulate materials to our advantage. For our technology to get better, faster, smaller and cheaper, the properties of materials must be better understood. Since blacksmiths began to experiment with heat and different metals, knowledge of the properties of metals has only increased. It was found that different elements have different melting points. When a metal is heated it is easier to shape, but when cooled was more difficult. Metal properties such as malleability, ductility, melting point, heat absorption, etc. were learned about. By mixing different elements different properties were obtained. One could make a metal stronger by mixing it with another metal. These mixtures are called alloys. These discoveries have been so important to a civilization's technology that historians have named different ages after the materials that the tools and weapons were made from. Following the Stone Age was the Copper Age followed by the Bronze (an alloy) Age, followed by the Iron Age. Today, as in ancient times, knowledge of the various properties of metals and metal alloys is necessary to be able to create tools.

1.1 Crystal Structure

One of the interesting properties of metals is that in their solid state they exhibit what is called a crystal structure. Crystal structure contributes to a lot of the properties that a metal has.

The three main crystal structures are called Body-Centered Cubic (BCC), Face-Centered Cubic (FCC), and Hexagonal Close Packed (HCP). Figure 1-1 illustrates the difference [1]. The black dots are locations of atoms, and lines drawn are to guide the eye and show the 3D nature of the structure. One important part to note is that this is shorthand for the basic structure of the crystal. The figures in Figure 1-1 are referred to as unit cells and are a summary of the structure. A unit cell is the smallest piece of a crystal you can grab and then repeat to recreate the crystal. A crystal will have these unit cells repeated in all directions. In solids, the typical spacing between nearest neighbor atoms is a few angstroms.

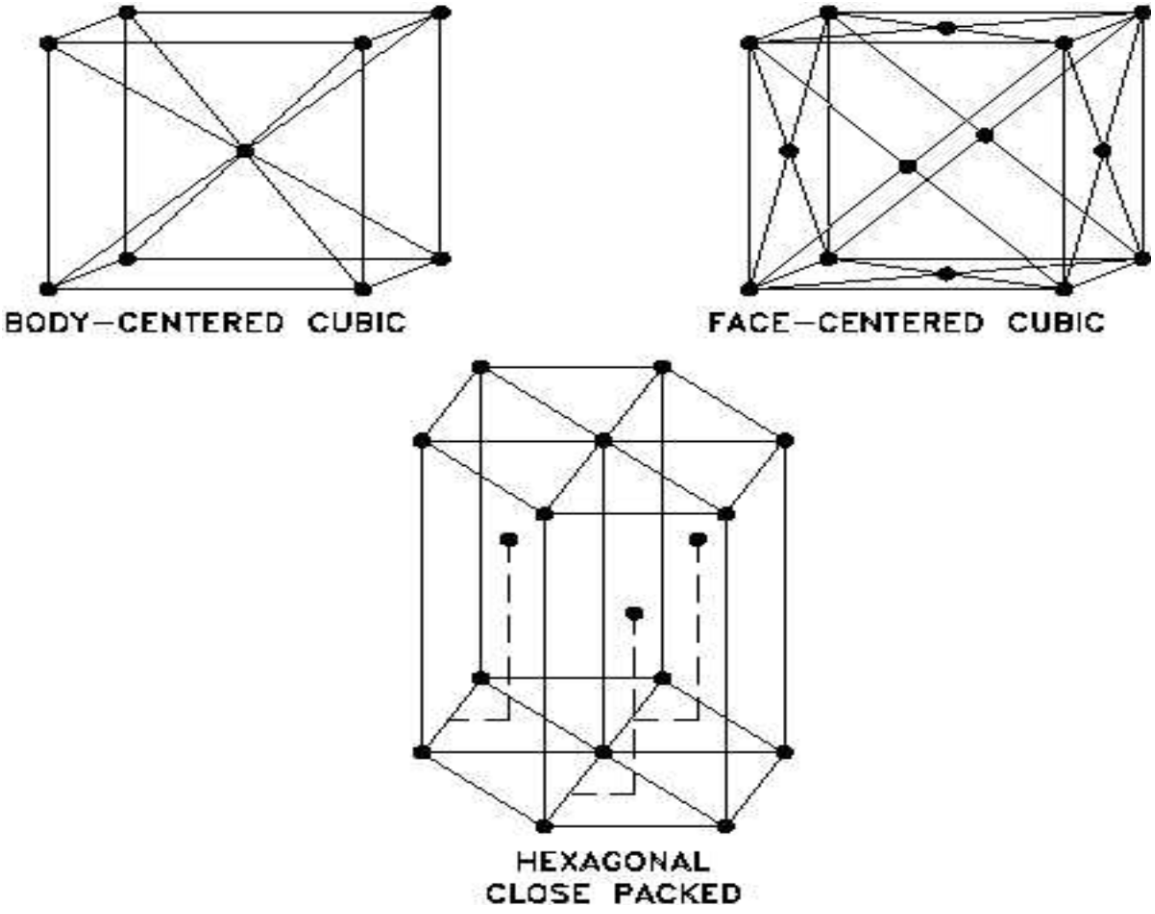

Figure 1-1 Crystal Structures

1.2 Ordering

In binary alloys things get interesting. The fact that there are two different atoms present in the solid changes the thermodynamics of the preferred crystal structures. In this study our main interest is in binary alloys that exhibit FCC structure (in terms of sites where atoms are found). If one were to look at our material and find that the atoms were randomly placed at each location this would be called disordered, even though it would still be an FCC crystal structure. If, however, there was a certain pattern to which atoms were at each location then this would be called ordering. There are different kinds of ordering, the one this research concerns itself with is called the $L1_0$ phase. $L1_0$ is when you have a binary alloy that has fifty percent one element and fifty percent another element, with the elements appearing in the positions indicated in Figure 1-2. Not all fifty-fifty(50/50) alloys exhibit the $L1_0$ structure.

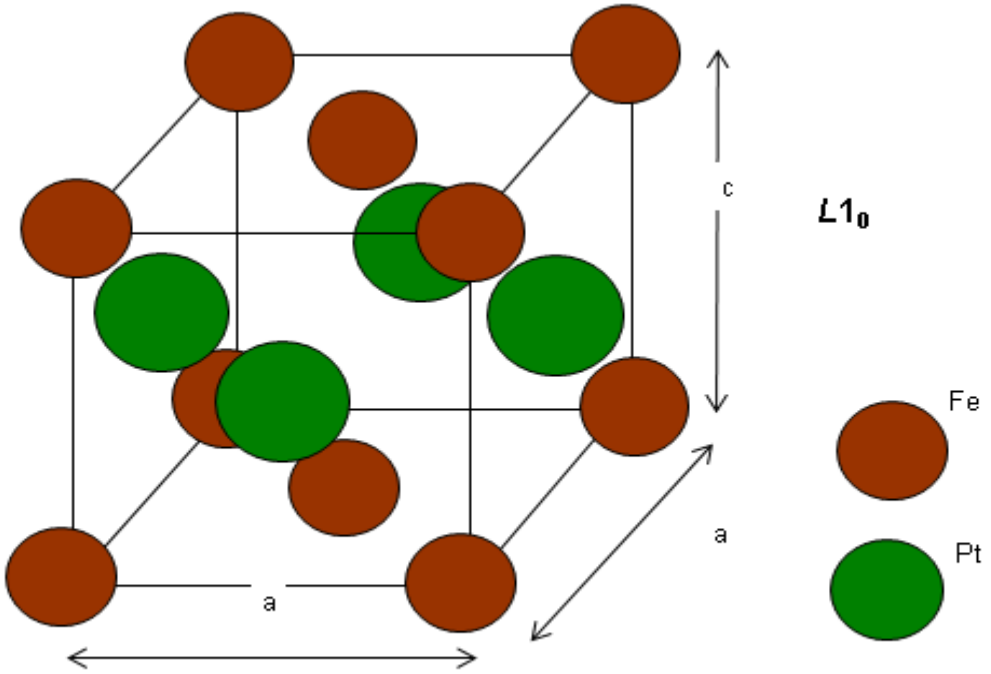

Figure 1-2 $L1_0$ FePt Ordering

1.3 Order-Disorder Temperature and the Kinetics Limit

Ordering is thermodynamically preferred if the temperature of the metal is below the order-disorder temperature. If the temperature of the metal is above the order-disorder temperature, then thermodynamically it will want to be in a disordered state. If this were the only thing influencing whether a given binary alloy is ordered, then a 50/50 mixture at room temperature will always be ordered. However that is not the whole story. If a metal is very cold the atoms won't have very much kinetic energy, therefore they will not be vibrating. If the atoms are not able to move around because their temperature is too low, then even if it is thermodynamically preferable to be ordered, a disordered state will not be able to order. The atoms will not be able to move to a location that is thermodynamically preferred. This is called kinetically limiting. There are two competing factors. If the temperature is too low, it will not order due to kinetics, and if the temperature is too high, it will not order due to thermodynamics [2–6].

Another part of the story is that the order-disorder temperature is different for each alloy. Comparing an FePt alloy to a NiPt alloy, the order-disorder temperature for one is higher than the other. For example, a study comparing NiPt with CoPt found that the order-disorder temperature for the NiPt was around 655 °C but the CoPt was around 827 °C [7]. This is interesting because cobalt and nickel are next to each other on the periodic table, and so should have similarities, yet the order-disorder temperature was different by over 150 °C.

1.4 Bulk vs Nanoparticles

Much research has been done on the order-disorder temperatures of alloys. The first work was done on what is now referred to as bulk material. This means a large quantity of material,

usually a few hundred nanometers in each direction. From a theoretical point of view one can assume that there are no boundary conditions, or that the boundaries are infinitely far away. Following this, work was done on thin films of material. This means that the material is relatively thin, tens to hundreds of nanometers, but still assumed to be large in the other two dimensions. What was found was that the order-disorder temperature is actually lower in a thin film than it is in bulk [8]. It seems then that the surface effects lower the order-disorder temperature. So the new frontier is finding the phase transition temperature of alloy nanoparticles. A nanoparticle is material that is smaller than 100 nanometers in diameter [9]. At this size the boundaries are much closer to each atom and the boundary effects cannot be ignored. It is theoretically predicted that the order-disorder temperature should be even lower for nanoparticles than it is for thin films [2, 3].

Currently, the exact temperature at which a binary nanoparticle undergoes a phase transition is unknown because there are so many variables that have an effect on said temperature. The exact composition of the alloy and the size of the nanoparticles have a direct relation to the order-disorder phase transition temperature. In general for a binary alloy, the closer to a 50/50 composition the higher the order-disorder temperature will be. Examples can be seen in the binary phase diagrams for bulk systems [10-11]. The smaller the nanoparticle the lower the order-disorder temperature will be [2, 3]. As an example, B. Yang et al. calculated a 3 nm particle will have a 20% lower order-disorder temperature than a 6 nm particle [3].

Size also has an impact of the kinetics. In the bulk, the kinetics limit is crossed when, within the volume of the sample, there is sufficient atomic hopping for long enough time to nucleate a stable seed particle of the new phase. Once a stable particle of the new phase is nucleated the subsequent growth can proceed with lower barriers. Thus, two important variables

that impact the kinetics are the temperature and length of time the particles are heated. When our nanoparticles are made, they are disordered. The samples must be heated hot enough and long enough to nucleate a stable ordered region within the sample. Stable ordered regions will only occur if the temperature is under the order-disorder temperature. The third important variable to impact the kinetics is size. Ordering begins when a stable ordered region is nucleated within the sample. For a given anneal time and temperature, when the sample volume is large the probability for nucleating a seed of the new phase is higher than when the sample volume is small. Thus, purely on the basis of particle size, one would expect nanoparticles to need higher temperatures or longer times to achieve substantial ordering. Irrespective of thermodynamic considerations, nanoparticles should be more difficult to order.

Chapter 2

Measuring Order-Disorder Temperature Experimentally

The properties of a metal, specifically a binary alloy, are different between a bulk material and a thin film, and different again for a nanoparticle. Knowledge of the properties of these materials is crucial to advance nanotechnology. Nanotechnology is a very big field, with many applications in military and non-military areas alike. Many devices need to operate in various temperatures. Having knowledge about exactly what temperature a phase change will occur for parts of a system will be very important. In general the research will add to the scientific community's knowledge about the order-disorder temperature of binary alloy nanoparticles.

One specific application is for magnetic data storage. Currently the hard drives of computers use grains (regions of a film) that have a magnetic moment [12]. Many of these grains together act as a bit of information. If the moment is one direction that would be a 1 and the other direction it would be a 0. However the current materials in recording technology, if made too small, tend to change direction randomly over time due to thermal fluctuations. This is a size effect where the energy per unit volume times the small volume of the particles is comparable to thermal energies. Current hard drive media uses a group of grains as a bit because it will be less likely for one to flip. The binary systems we are studying (FePt specifically) have a sufficiently high energy per volume, that even particles on the few nanometer scale would not flip at reasonable ambient temperatures. Our research will aid in the understanding of the ordering state

of these nanoparticles, which may enable computers to use one particle per bit, increasing data storage ten-fold. Our research aims to find the order disorder temperature for nanoparticles under ten nanometers. The smaller the particles, the more that can fit on a hard drive, and more data storage will result.

Our goal was to experimentally measure order-disorder transitions in binary alloy nanoparticles. This goal included the order-disorder temperature as a function of size and the ordering state (a property known as order parameter) as a function of temperature. One desire was to directly observe (in-situ) the order-disorder transition in nanoparticles. Our focus is $L1_0$ phase systems, for example alloys such as AuCu, FePt, NiPt, CoPt. There were several practical needs in this study. First, ordered particles had to be produced that had a theoretical order-disorder temperature within the temperature range of our equipment. Second, suitable substrates and sample preparation methods needed to be determined and perfected to allow an in-situ temperature study. We were not able to perform an in-situ temperature study. We were, however, able to produce ordered nanoparticles (FePt and FeNiPt), and a suitable capping layer was found (alumina). In addition we were able to show the size dependence of the order-disorder temperature for FeNiPt particles.

2.1 Ordered Particles

It had been proposed to determine sample ordering by observing the electron diffraction pattern in the Transmission Electron Microscope (TEM). An approach to finding the order-disorder temperature of a sample is to begin with a sample that is ordered, heat the sample up while it is in the TEM (in-situ) under observation, and then watch for the change in the diffraction pattern. A hot-stage allows us to controllably heat the sample in the TEM and thus directly observe the transition. To do this, an alloy would be needed that would allow easy

creation of ordered nanoparticles but also had a theoretical order-disorder temperature within range of the in-situ equipment.

2.2 Sample Preparation: Compositional Changes in Processing

A literature search for many different binary alloys was carried out. Specific attention was paid to binary alloys whose order-disorder temperature is within the range of our hot-stage (below 1000 °C). Alloys found include NiPt, AuCu, and CoPt. As the nanoparticles will have a lower order-disorder temperature than for bulk, these should all be within our desired range. However, our group already had preliminary data on NiPt and AuCu which did not order as nanoparticles. As these anneals were done under the bulk order-disorder temperature, this lack of ordering is likely due to either not having enough kinetics (low nucleation density in nanoparticles) or size lowering of the order-disorder temperature. The annealing temperature needs to be above the kinetics limit but below the order-disorder temperature. While there is some connection between the kinetics limits and the elemental composition, for similar systems one would expect the kinetics requirements to be similar and insensitive to specific composition (ie, FePt vs. NiPt). Thus, a lower order-disorder temperature alloy should result in a smaller processing window (the temperature difference between kinetic limit requirements and order-disorder temperature). It is not unreasonable to imagine materials where in the nanoparticle form, the kinetics temperature limit is higher than the order-disorder temperature. In fact we believe this to have happened with NiPt nanoparticle samples we have made where ordering was never achieved. The kinetics limit requirements for nanoparticles is a complicated question where the temperature and length of time to anneal must be experimentally determined for the alloys and particles in question. A related concern is particle growth where the anneal changes the particle size making it more difficult to compare differing times and temperature of anneal.

Since they did not order, NiPt and AuCu were not used in this study. Our FePt samples did order; however, their theoretical order-disorder temperature (~1300 °C [11]) is higher than our hot-stage is able to go (~1000 °C). To get around this problem it was proposed to use a pseudo-binary alloy (FeNiPt), in which there is fifty percent of one element (platinum) and the other two elements (iron and nickel) are varied. For example one could have fifty percent platinum, ten percent nickel and forty percent iron, and another sample of fifty percent platinum, twenty-five percent nickel and twenty-five percent iron. When this type of variation is done for bulk alloys, the variation of the order-disorder temperature with composition is linear [13-17]. For this work, we also assume the order-disorder temperature variation is also linear for nanoparticles. In this manner one should be able to decrease the theoretical order-disorder temperature of the FePt by mixing in more and more nickel. With the right composition one could have a sample whose order-disorder temperature is within the in-situ limits.

Earlier work by our team has shown that controlling the final composition of the nanoparticles is difficult. Phase diagrams for bulk metal alloys show that for most binaries the highest T_{od} is when the atomic percent composition is close to 50/50. We have had difficulty obtaining consistent nanoparticle compositions close to 50/50. According to the Rutherford Backscatter Spectroscopy (RBS) done at UCF by our collaborators, the samples should be close to 50/50 as intended. Yet when the samples were annealed and prepared our FePt and AuCu samples were not what they should have been.

Early difficulties with composition arose because of reactions with the substrate. In FePt samples, the Fe would react with the SiO_2/Si substrate to form iron silicide. For FePt and the pseudo binaries of NiFePt, this problem appeared to be fixed by introducing water vapor into the annealing gas to counterbalance the reduction due to hydrogen and the oxidation by H_2O [18].

When the particles are well reduced in just hydrogen, the Fe appears to be free to diffuse into the substrate. Some low level of oxidation on the surface appears to keep the Fe retained to the nanoparticle. For the AuCu system, we believe composition problems to arise during tripod polishing, see section 4.3.2. We propose using capping layers to limit surface exchange of atoms to address these problems.

2.3 Sample Preparation: Capping Layers

An exploration of capping layers was undertaken to address both compositional variations and particle growth. A way to limit the particles' growth during anneals was needed so that an anneal could be done for the amount of time needed to create ordered particles but without extensive particle growth. In addition a way to prevent composition variations was required. Particle growth arises due to Ostwald ripening [19], where particles exchange atoms by diffusion across the surface between then. The lower energy or larger particles will grow at the expense of the higher energy smaller particles. With two elements in the particle compositions, there is a possibility that diffusion rates, diffusion lengths, and size related stabilities could differ between elements and result in compositional differences between particles. Our attempt to impact or control these issues was by coating our sample with a capping layer before annealing. Suggested coatings were carbon or alumina.

Carbon is a common conductive sample coating layer for TEM and SEM imaging. However, alumina is not electrically conductive. This is problematic for TEM observation because of charging. The electron beam used by the TEM will knock a significant number of electrons from the sample (called secondary electrons) leaving the viewing area positively charged. If there is a reasonable connection to electrical ground, the excess charge is neutralized by the flow of charge from elsewhere. If the sample is non-conductive it cannot discharge to

ground and the viewing area becomes charged. In this case the images become distorted and in many cases the local charging damages the sample. However, in some situations a sufficiently thin layer of non-conductive material will still allow sufficient conduction or tunneling to the more conductive substrate that charging will not cause extensive problems.

A second concern is the possibility that during the high temperature anneals, the elements in our nanoparticles could have a reaction with the capping layer or the substrate. This would impact both the composition and the broader thermodynamics and kinetics of the particles. Ideally we hope to find a capping layer and substrate that would have minimal impact on the particles.

If a capping layer is used, one appealing option is to deposit our nanoparticles onto a salt substrate. In this case the salt can be dissolved in water and the capping layer film, with nanoparticles trapped in the layer, can be scooped off the water's surface onto a TEM grid. This is a very quick and easy sample preparation method. However the melting point of some salts is an issue. For example, NaCl is 801º C, so anneals could not be done higher than that. An additional difficulty is that the alumina deposition system also supports semiconductor processing, and as a result is not supposed to have sodium or potassium inside the chamber. This limits our substrate options if an alumina layer for capping were to be used. Other salts that are not Sodium or Potassium based are generally difficult to work with for safety reasons, financial reasons, or practical reasons. NiPt, FePt and FeNiPt on salt were not used due to needing an anneal close to the melting point of salt (801 °C). Only AuCu on salt was used because AuCu needs a much lower anneal to achieve ordering.

Chapter 3

Method and Procedures

Work began by analyzing NiPt and FePt nanoparticle samples. It was found that none of the NiPt samples that had been made and annealed (below the 660 ºC bulk order disorder temperature [10]) had ordered. Samples were verified to be within the correct composition and size range. Kinetic factors were assumed to be the limiting factor for the lack of ordering as evidenced by the work on FePt. For the FePt samples only those that had been annealed at 700 ºC for 30 min and 800 ºC for 30 min had ordered. This indicates that the kinetics limit for these binary alloy nanoparticles is around 700 ºC. FePt has a T_{od} that is too high for our proposed in-situ study. However, samples of pseudo binary FeNiPt had previously been prepared with the NiPt and FePt samples that would have acceptable T_{od}. Additionally, plans were made to create samples that should order and be more accessible to the temperature limits for the in-situ study. I went to UCF to work with our collaborators to produce samples of FeCoPt, CoPt, and AuCu. Samples were made on different substrates so that multiple options were available. Substrates used were; salt, silicon wafers with SiO_2 layers, and MgO. FeCoPt was made by keeping Pt close to 50% while varying Fe/Co ratios. CoPt and AuCu samples were also made, keeping compositions close to 50/50.

While at UCF, pieces of sample were annealed to overcome the kinetics limit and get the particles to order. Later our collaborators at UCF annealed more pieces at different temperatures

to better understand the kinetics limit. Phase diagrams for bulk materials were used to guide choice of annealing temperatures.

Most of the samples for TEM were prepared by a technique called tripod polishing. There were some unusual results so some samples were also prepared by a Focused Ion Beam (FIB) technique. Data was taken in the TEM, such as particle size, particle density and distribution, the presence of ordering, and the chemical composition.

The remainder of chapter 3 contains more detailed information on each step in the process. The Vanfleet research group has several in-depth tutorials for more information on each of the following sections.

3.1 Substrate Preparation

Samples on three different substrates were made: salt, MgO, and silicon wafers. The MgO substrates came already prepared. The MgO pieces are a square centimeter by a millimeter thick. The salt starts out as one large piece. One places a razor blade on the salt (aligned to the cleavage planes) and gives the blade a tap with a heavy object to cleave the salt along a cleavage plane. One should then have a thin piece of salt that is flat and smooth, about the same size as the MgO pieces. The silicon wafers are [100] wafers that were placed into an oxygen or air environment and heated so that a silicon oxide (SiO_2) layer is formed. The length of time in the oven dictates the thickness of the layer. Our SiO_2 layers were grown to be between 10-30 nm thick.

3.2 Sputtering

Sputtering is a deposition technique commonly used in the creation of thin films. The technique involves shooting an ion beam at a material such that the atoms from the material are

knocked off and end up getting deposited everywhere inside the chamber, including onto the sample. This is usually done in a vacuum to prevent the formation of metal oxides. The part that shoots the ion beam is called the gun, and the material that is hit with ions is called the target. Co-sputtering is a technique that has multiple guns and targets in the sputtering chamber operating at the same time. For example, AuCu can be made by having a gold target with a gun hitting it, and a copper target with a different gun hitting it. For CoNiPt, there would be three guns and three targets. The deposition rate (amount of material deposited over time) is a function of the power delivered to the gun, the distance from material to target, and the composition material of the target. For example, less power is needed to sputter gold than platinum. In addition, not all guns operate with the same efficiency. Also, the distance from sample to target affects the deposition rate. These factors mean that every time a gun or target is changed the system must be recalibrated. This is done by making a few calibration samples. Guesses are made for the wattages on the guns based on previous experience. A long enough deposition is done to have a few hundred nanometers of material. Ellipsometry is then used to measure the total thickness. Rutherford Backscattering Spectrometry is used to measure the compositions of each of the alloys. Then a deposition rate for that wattage is calculated. Once a few deposition rates are obtained for different wattages one assumes a linear relationship and sets the wattages to produce the desired compositions. Sputtering is done for a short enough time to get sufficiently thin depositions that either form nanoparticles from the deposition conditions or the thin films break up into particles upon annealing.

3.3 Capping Layers

Capping layers were not always used when preparing samples. Two different kinds of capping layer were tried, carbon and alumina. This was an attempt to prevent some of the composition problems in our early samples, and particle growth during annealing.

3.3.1 Carbon

Carbon was deposited using evaporation. A piece of graphitic carbon was heated by running a current through it. When hot enough the carbon starts to evaporate off the graphite. Two different deposition systems were used, one is a Denton Vacuum evaporator (DV-502A) and another is a Quorum Turbo-Pumped sputterer (Q150T ES). It was found that for our needs the sputtering system worked better. It produced layers of carbon whose thickness did not vary as much. It was also easier, faster to use, and more reliable.

3.3.2 Alumina

Alumina is aluminum oxide (Al_2O_3). The technique used is called reactive sputtering. This is a setup just like that described in the sputtering section 3.2, only instead of using an alumina target (for the desired film), an aluminum metal target was used. At the same time, oxygen is deliberately flowed into the chamber during deposition to react with the metal aluminum to deposit aluminum oxide (alumina). Ellipsometry was used to determine if our alumina layer was thick enough and didn't have holes in it.

3.4 Annealing

Annealing is done by placing the sample in a quartz tube. Then a gas is made to flow through the quartz tube. Most often an argon carrier gas was used with an addition of hydrogen

to create a reducing environment. For some of the samples, water vapor was put in the gas by bubbling it through water in a flask. This prevented iron movement from the particles to the substrate that resulted in silicide formation in the silicon substrates and a deficiency of iron in the particles. The gas that flows out of the quartz tube is run through a flask of oil to prevent back flow of gas. The quartz tube is heated in a furnace to the desired temperature and held at that temperature for the desired time. See Figure 3-1.

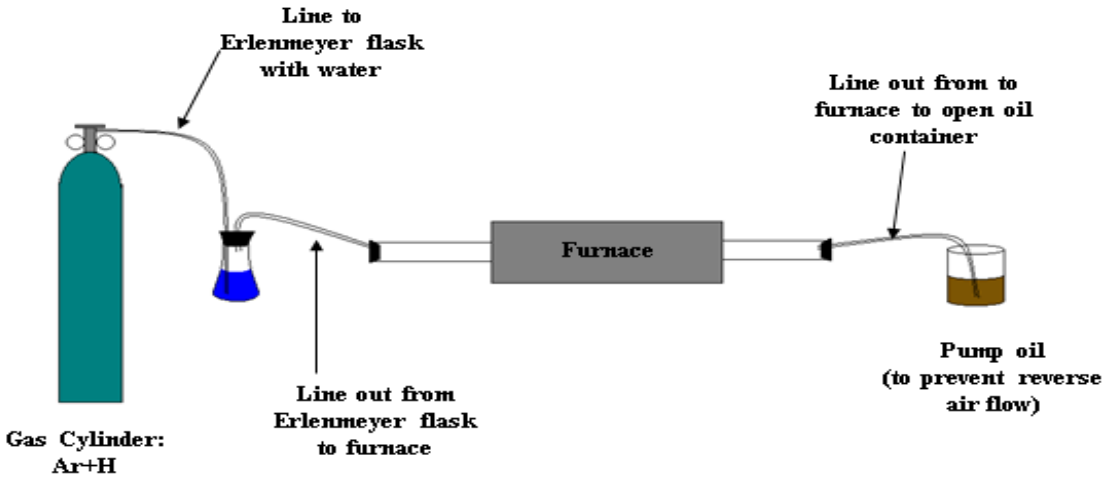

Figure 3-1 Annealing Furnace Setup

3.5 Sample Preparation

At this point in the process samples were prepared for the Transmission Electron Microscope (TEM). TEM samples needed to be thin (typical goal is less than 100 nm thick) and preferably 30 nm or less. Most of the samples that were prepared on silicon substrates were polished using the tripod polishing technique. Samples that were made on MgO substrates or

NaCl substrates were not used in this study. One sample was also prepared with a Focused Ion Beam (FIB) technique.

3.5.1 Tripod Polishing

We begin by cleaving a piece of our silicon wafer with nanoparticles on it using a diamond scribe. The piece is then washed with acetone and methanol and mounted to a glass post with wax. The sample is mounted with particle side down in the wax. The glass post is attached to two 'feet' that are controlled by micrometers to be able to change the height of the feet. The back feet are raised higher than the glass post, then the whole assembly is turn upside-down and placed on a polishing wheel. The polishing wheel has a diamond lapping film placed on it. The diamond lapping film has diamond particles stuck to the surface to be able to remove material. This is like sandpaper. As with sandpaper a high grit lapping film is used first and progressively changed to finer and finer grits. The glass post and two 'feet' are referred to as a tripod and the removal of material is called polishing, hence the name tripod polishing. Since the back feet are higher than the glass post, when polishing is done the sample will be in a wedge shape. See Figure 3-2. Due to this geometry the finished sample edge can be sufficiently thin for TEM study. The sample is then removed from the tripod by dissolving the wax that holds it. The sample is rinsed in acetone and methanol to remove any remaining wax and the sample is mounted to a TEM grid with an adhesive. After letting the sample sit overnight the adhesive is cured by putting the sample on a hotplate for 5 minutes. The hotplate temperature is around 100º C.

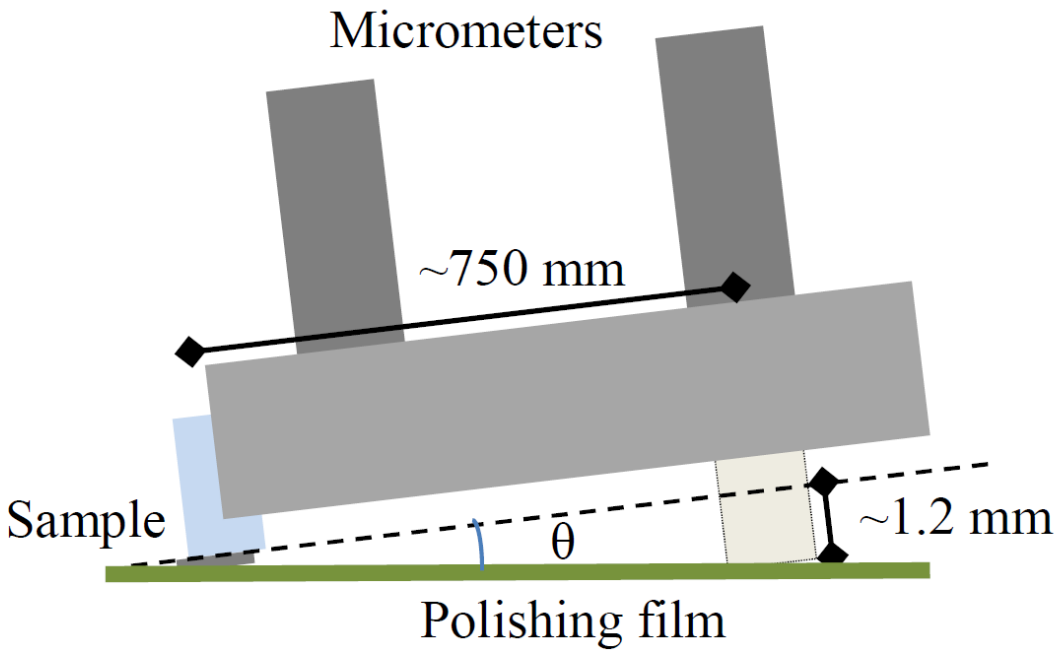

Figure 3-2 Tripod Polishing

3.5.2 Focused Ion Beam

The Focused Ion Beam (FIB) is a difficult technique that takes many hours to prepare one sample. First, a piece of sample is cleaved with a diamond scribe. The sample is mounted to a post and put into the FIB, which is a Scanning Electron Microscope (SEM) with a scanning ion gun. We used a standard FIB in-situ liftout procedure where a section of the sample is partially thinned and cut free with the ion beam, it is moved and attached to a grid using an in-situ omniprobe needle, and then final thinning is carried out in selected areas. There is however an important variance in the standard process for this sample. As the area of interest is at the exposed surface, thinning of the sample is only done on the non-nanoparticle side of the sample.

3.5.3 Salt Substrate

If a salt substrate is used a capping layer must be done after particles are deposited and before preparation for TEM can begin. Then one can place the sample on a wire mesh in a container and slowly raise the water level to dissolve the salt. The carbon film will float on top of the water's surface and the particles will be embedded in the carbon film. Then a TEM grid could be taken with a pair of tweezers and used to 'scoop' the carbon film onto the TEM grid.

3.6 TEM Data Acquisition

The sample preparation techniques mentioned are done so that our sample is thin enough to be seen with the electron beam of the TEM. Since our nanoparticles are already very small (around 10 nm) the quality of samples is crucial to be able to have signal above background. If the sample is too thick, data will not be able to be taken with the TEM, or will not be of very good quality. This is why the sample preparation techniques need to be of a very high quality. The samples which have been mounted to a TEM grid are placed into a TEM grid holder. Then the grid holder is placed into the TEM.

3.6.1 Images

Images are used for the purpose of measuring the size of our particles. Figure 3-3 is an example of what can be seen. Using the microscope software the diameter of individual particles can be measured and average particle sizes can be found. Boxes were drawn around an area and the number of particles in that area were counted. With these two pieces of data an equivalent thickness was calculated to see how much material there is. Equivalent thickness is calculated by using the average diameter to find an average volume assuming spherical particles. Then the average volume is multiplied by the number of particles in the area. The total volume is divided

by the area those particles are in to get the equivalent thickness. This is done so that if two samples have different size particles or distributions comparisons between the amount of material can still be made.

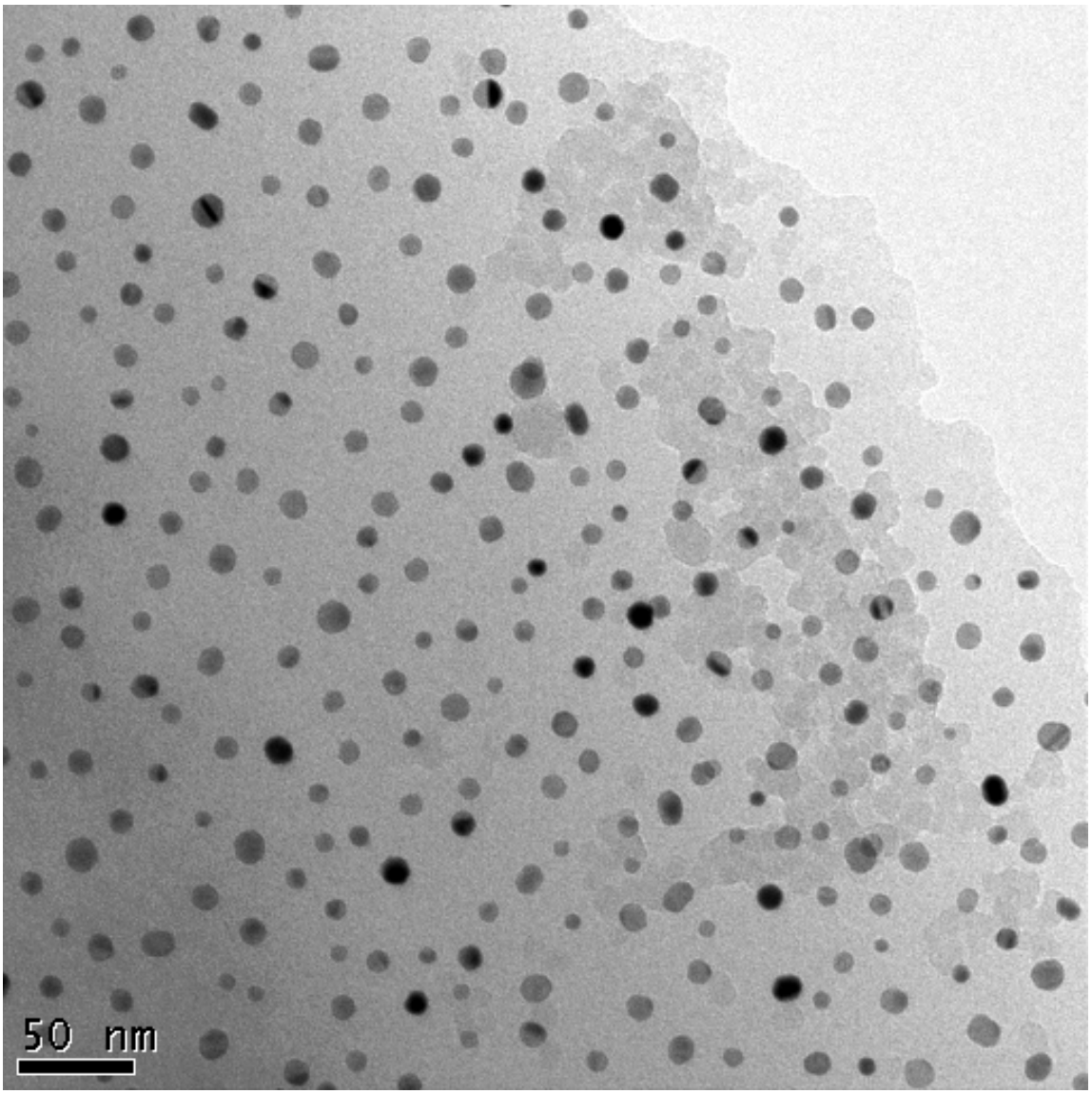

Figure 3-3 TEM Image of FeNiPt Nanoparticles

3.6.2 Diffraction

A diffraction pattern is used to determine whether our nanoparticles have ordered. The silicon substrate makes a diffraction pattern because it has a diamond cubic crystal structure that exhibits a pattern similar to the FCC crystal structure of the particles. The nanoparticles will also make a diffraction pattern because they have a crystal structure. In a disordered particle this diffraction pattern is FCC but in an ordered particle it is similar to an FCC with some extra features due to the ordering. The diamond cubic structure of the silicon substrate and the FCC like structure of the nanoparticles is similar. However, the spacing of the lattices is different for the silicon substrate than it is for the binary alloy of the nanoparticles and therefore enables us to distinguish between the two in the diffraction pattern. Also since there is more silicon material than nanoparticle material the silicon diffraction spots will be brighter than those from the nanoparticles. This is why it is so important to have thin samples, otherwise the spots from the substrate will be so bright they will drown out the pattern from the nanoparticles. In a very good sample, there is little or no evidence of the silicon substrate in the diffraction pattern. Another thing to consider is that each nanoparticle can be oriented differently than the substrate and from each other. This causes the nanoparticles to make rings of intensity in the diffraction pattern rather than spots. The rings are made up of many spots. The substrate diffraction pattern, if seen, is a single array of spots and does not form rings. Certain rings are always present due to the crystalline nature of the nanoparticles. When there is ordering present, there are additional rings in the diffraction pattern. In Figure 3-4 arrows have been added to the left diffraction pattern to aid the eye in seeing the bright spots that are part of the ring that indicates ordering. This is what is used to determine if ordering is present.

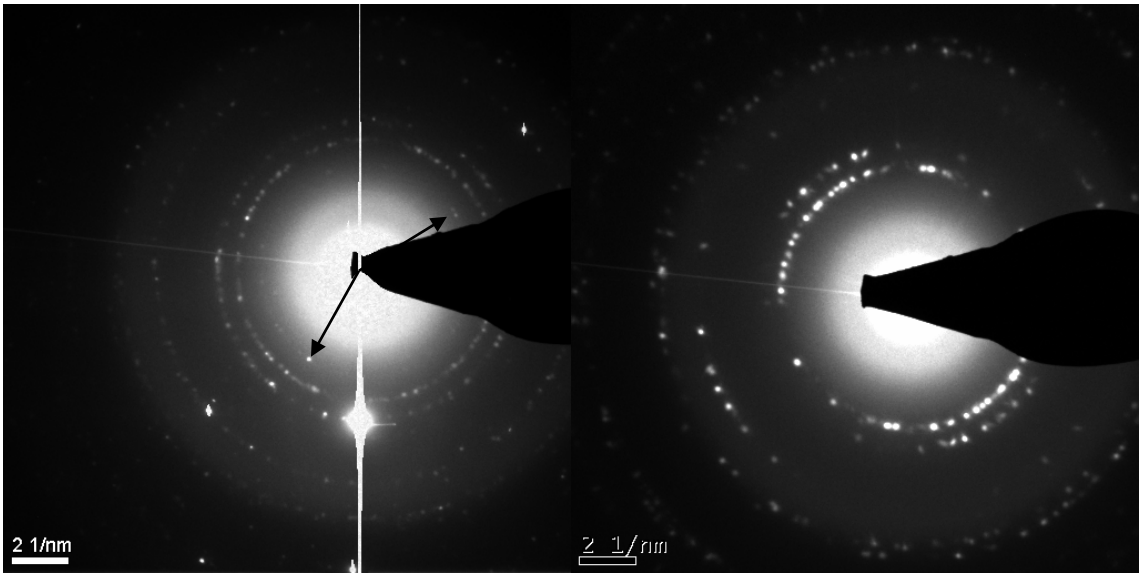

Figure 3-4 Ordering (left) vs No Ordering (right)

3.6.3 Energy-Dispersive X-Ray Spectroscopy

When the electron beam passes through the sample, the electrons have a chance of interacting with the electrons in the atoms of the material in our sample. If the electrons from the electron beam knock an electron from an inner orbital completely away from the atom, an electron from a higher orbital will fall down to take its place. When this happens that electron that falls down will release a photon of energy equal to the energy difference between those orbitals. The energy difference between orbitals is well quantified for almost every element in the periodic table. Energy-Dispersive X-Ray Spectroscopy (EDS or EDX) uses this to determine the atomic composition of samples in the TEM. Most of the photons happen to be in the X-Ray spectrum. An X-Ray detector is put near the sample to measure the energy of the photons coming off the sample. The different electron shells are associated with different energy levels. There are K-edges, L-edges and M-edges. Because of the energy range of our detector k-edges were used to quantify Co, Cu, and Ni. L-edges were used to quantify Au and Pt. Without

additional data beyond the spectra, one cannot know exactly how many atoms of a particular element there are in the sample. However, one can use the relative comparison between peaks within the spectra to quantify the relative amount of elements in the sample. There are several processing and correction steps that must happen for this relative correction to be made. These processing steps include removal of background counts, correction for detector efficiencies, and correction for differences in the "electron in to x-ray out" (k factors) efficiencies for each element. Figure 3-5 is an example of a spectrum before and after background subtraction in preparation for quantification. The important data are counts above background for the x-ray peaks of interest. For low x-ray energy the detector has low collection efficiency (absorption of the x-ray prior to collection in the active region of the detector) and at high energies the collection efficiency also drops (high energy x-rays pass through the active detector region without being collected). Corrections are made to account for these detector inefficiencies. Since our peaks of interest are in the middle of the detector range, these detector corrections are small. The corrections for element and transition edge are called k-factor corrections. The quantification software multiplies the number of counts detected, by the detector correction and by the k-factor correction to predict the actual number of counts given off. Once this is done for two elements, a ratio of counts can be made. Typically, k-factor error is dominant in this quantification approach and is typically quoted as around 5% for K-edges and 20% for L-edges [20]. Our group has independently measured the k-factor for the Pt L-edge with FePt nanoparticles in comparison to RBS results and thus we feel the Pt L edge error on the k-factor is less than the quoted 20% [21]. In practice, measured compositions from spot to spot vary at best by several percentage point (on the order of effect due to the k-factor error) in compositionally stable samples e.g. FeNiPt and at worst many 10's of percent in poor stability samples.

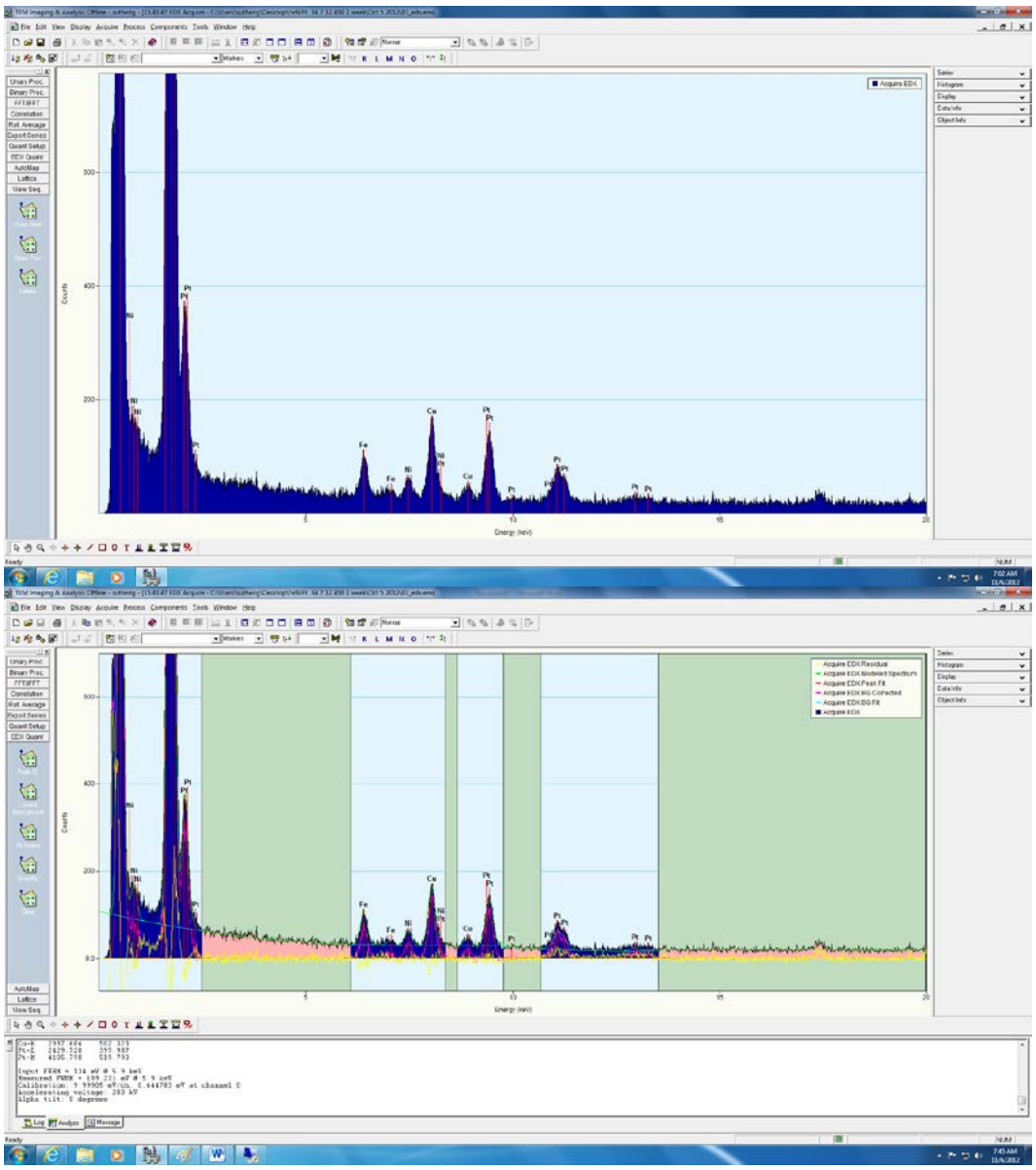

Figure 3-5 EDS: Unprocessed Spectra (top) and Processed Spectra (bottom)

Chapter 4

Data and Analysis

Here we present our data and conclusions. NiPt, FePt, FeNiPt, CoPt, and AuCu data series are discussed. A capping layer was found that can limit particle growth during annealing. In addition this capping layer seemed to fix composition variances. Alumina, rather than carbon, will suppress particle growth.

4.1 NiPt and FePt

Our research began with NiPt and FePt nanoparticles. Initially the NiPt samples were annealed at 600 and 500 °C for 30 minutes. This was because the T_{od} for bulk NiPt is around 660 °C [10]. No ordering was found, so anneals were performed at 550 and 650 °C for 24 hours and 450 °C for 1 week. No ordering was found in any of these samples. FePt samples were annealed at 800 and 700 °C for 30 minutes, as well as 550, 650, and 700 °C for 24 hours. The samples that were annealed at 800 °C showed ordering and those at 700 °C had fainter but still clear signs of ordering. However, even 24 hour long anneals at 650 °C and below were not sufficient to order these FePt nanoparticles. All these temperatures are well below the bulk T_{od} and well below all predictions of the size lowered T_{od}. Therefore, the thermodynamic driving force should have been large and by purely thermodynamic considerations they should have ordered. The obvious explanation for ordering at 700 °C but not at 650 °C is that the kinetics limit for these particles with moderate annealing times is between these two values. We conclude from these results that the kinetics limit is between 650 °C and 700 °C. As Ni and Fe are near neighbors in the periodic table and are similar in some properties, we propose they would have similar kinetic factors. Thus, similar kinetic factors for NiPt and FePt would mean that ordering for NiPt nanoparticles

should be impossible. This is because the anneal temperature must be below the T_{od} (660 °C for bulk [10]) but above the kinetics limit (between 650 °C and 700 °C).

It is for this reason that pseudo binary alloys were studied. Our NiPt and FePt work indicated that the processing window for NiPt is closed. Also the FePt order-disorder temperature is too high for our hot stage. By varying the ratio of iron to nickel one should be able to control the order-disorder temperature while keeping above the kinetics limits. We hypothesized that the relationship between T_{od} and composition would be linear. That is, if our FeNiPt is more iron than nickel it should be more similar to FePt. Similarly if our FeNiPt was more nickel it should be more similar to NiPt. In this manner samples can be created that have T_{od} below our hot-stage range but still above the kinetics limit.

4.2 FeNiPt

According to previous work, bulk NiPt should have a T_{od} of 660 °C [10] and bulk FePt should have a T_{od} of 1300 °C [11]. Five compositionally different FeNiPt samples were created. The samples we made were as follows (%Fe/%Ni/%Pt): 12.5/37.5/50, 16.6/33.3/50, 25/25/50, 33.3/16.6/50, 40/10/50. All 5 different compositions were annealed at three different temperatures for 30 minutes, 750 °C, 800 °C, and 900 °C. Three out of five compositions for FeNiPt ordered at all three temperatures, see Figure 4-1. We added the 660 °C and 1300 °C bulk T_{od} for the NiPt and FePt respectively to Figure 4-1. A trend line between these two points was also added to show the expected linear relationship between composition and T_{od}.

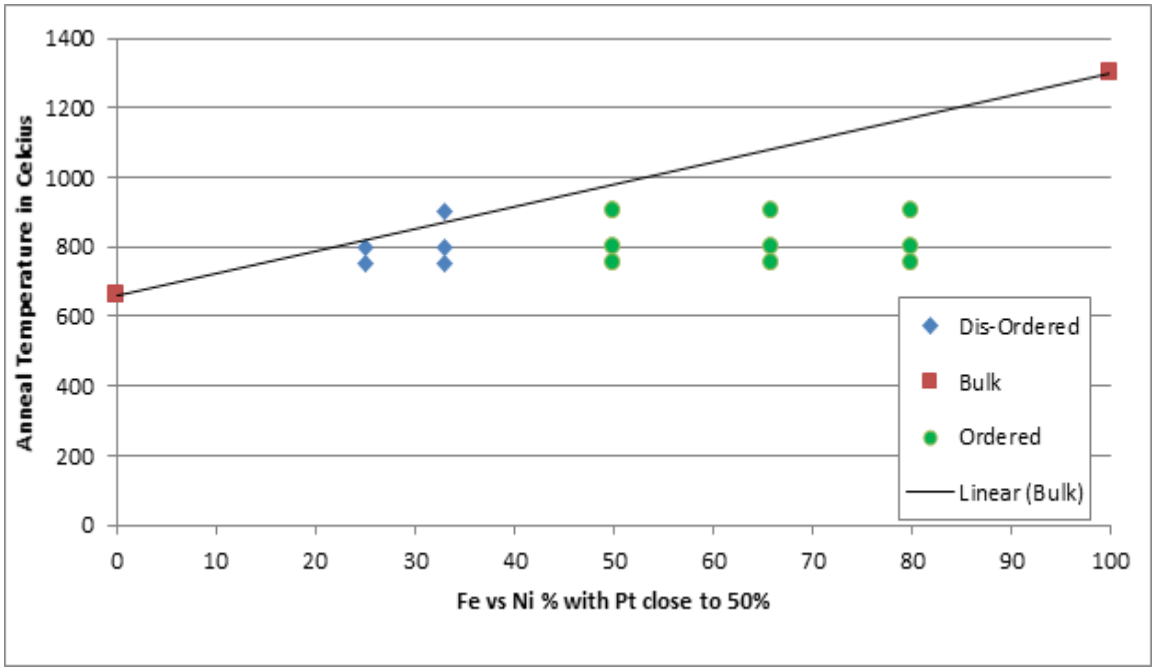

Figure 4-1 FeNiPt Ordering vs Non-Ordering

The hope for Figure 4-1 was that a given composition would show low temperature anneals that ordered and higher temperature anneals that did not. By shifting the linear T_{od} line downward, to account for size effect lowing, to a spot between the ordered and disordered point the size effect might be clear. However, this representation fails to include the important variable of particle size. Larger particles, due for instance to higher annealing temperature, should have higher T_{od} [2]. As expected, the higher temperature anneals had higher average diameters, as seen in the data in Figure 4-2. Figure 4-3 shows that there are no significant differences for different anneal temperatures in the compositions of the particles. Thus, material is not being lost to the substrate during anneal [18] but the particles are growing in size.

FeNiPt in atomic %	Average Diameter(nm)			Distribution(#/nm^2)			Equivalent Thickness(nm)		
	750C	800C	900C	750C	800C	900C	750C	800C	900C
12.5/37.5/50	5.72	8.35	10.8	0.00688	0.0036	0.0014	0.675	1.10	0.928
16.5/33.5/50	5.66	7.74	10.0	0.0075	0.00306	0.0019	0.710	0.744	1.00
25/25/50	5.89	9.03	9.93	0.0068	0.0028	0.0019	0.728	1.08	0.975
33.5/16.5/50	6.07	9.79	10.4	0.0056	0.0019	0.0014	0.654	0.933	0.815
40/10/50	6.01	10.9	10.8	0.0072	0.00296	0.0014	0.819	2.02	0.927

Figure 4-2 FeNiPt Sizes for Various Compositions and Anneals

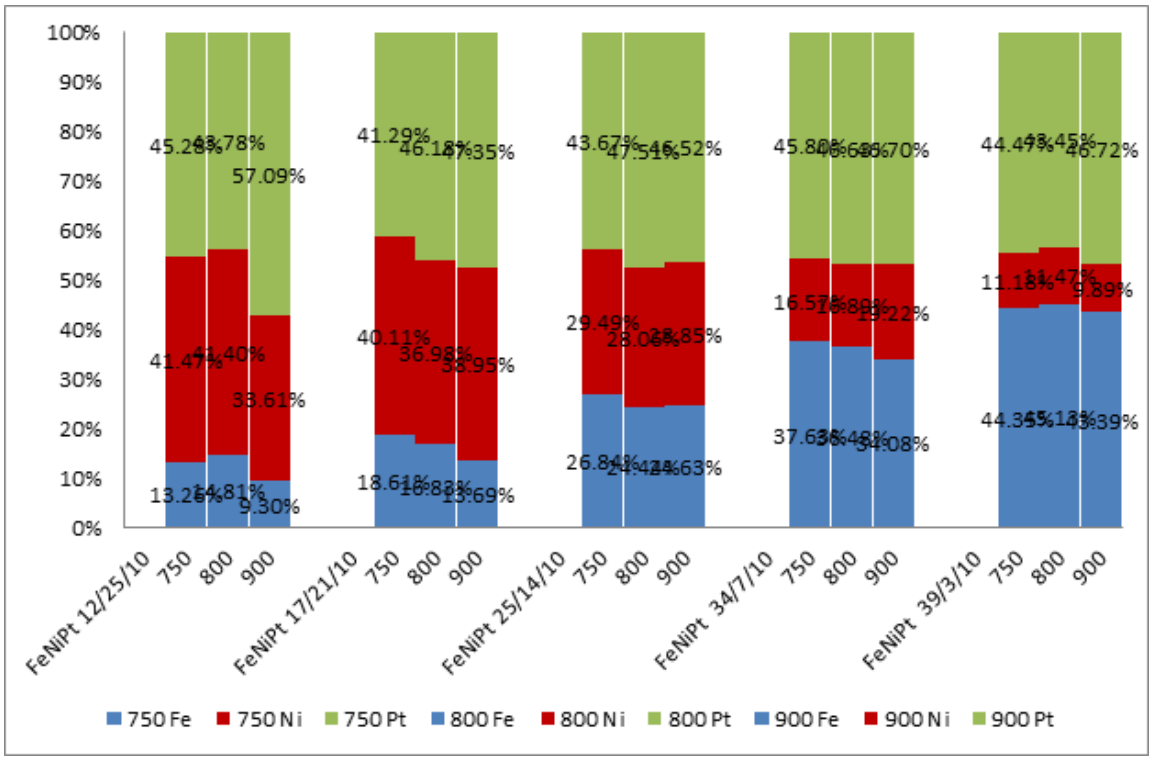

Figure 4-3 FeNiPt Compositions for Various Anneals

We propose the following approach to representing the data, as shown in Figure 4-4, that will show the effect of particle size on the thermodynamic order disorder temperature. The struggle is to decouple the particle size and particle composition. To do this we reference the anneal temperatures to the compositionally appropriate order disorder temperature. A ratio is

made of the anneal temperature divided by the theoretical T_{od} for bulk for that given sample composition. By using this ratio we are taking into account how the composition changes the T_{od}. We assume a linear relationship between NiPt and FePt compositions as shown in Figure 4-1. That ratio is plotted on the vertical axis and the particle size for that sample is on the horizontal axis. Sample ordering is coded by color and shape. For any ratios above one we expect to have no ordering occur (because we annealed higher than the theoretical T_{od} for bulk). Three lines were added to the figure to aid the eye. The first line is at a ratio of one showing the bulk limit. The second connects the two highest samples that ordered (small dashed) and the third is at the same angle and goes through the lowest ratio that did not order (large dashed). From this figure it is clear that there is a shift down in the T_{od} compared to the bulk for nanoparticles and that the shift is larger for smaller particle sizes. For particle sizes near 6 nm in diameter there is a shift of 10 to 15 percent, and for particles near 10 nm in diameter there is a shift of 0 to 6 percent. As mentioned in section 3.6.3 the error for composition is about 5 percent. This compositional error corresponds to a T/T_{od} error of about 5%. The error for particle size is also around 5 percent (0.15-0.5 nm). A single set of error bars were added for reference to Figure 4-4 in the upper left corner. All the data points have approximately the same error and inclusion of error bars on all data points cluttered the figure. This method of data analysis is new and shows some quantitative results that have not been seen before.

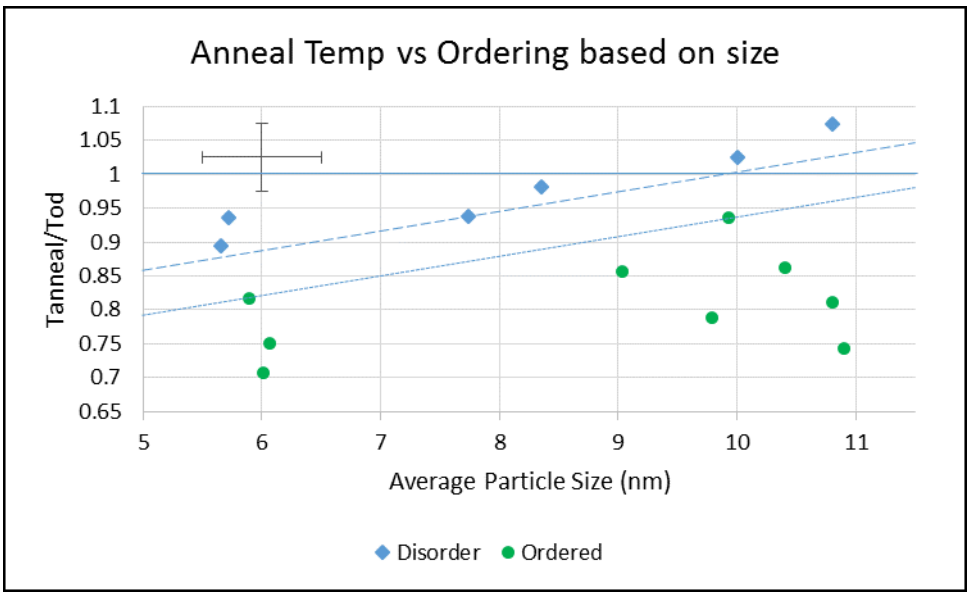

Figure 4-4 Anneal Temperature vs Ordering based on size

4.2.1 CoPt

Since the Fe rich FeNiPt particles would still theoretically have a T_{od} too high for our hot-stage, CoNiPt samples were made. The hope was to find a platinum alloy with a T_{od} lower than FePt to begin with, and then mix in nickel to lower the T_{od} even more. CoPt and CoNiPt samples were made. However there was no ordering seen for CoPt. This means that it is highly unlikely that any ordering would be seen in the CoNiPt samples.

4.3 AuCu

The T_{od} for AuCu in bulk is much lower than that for FePt or NiPt. The T_{od} for bulk AuCu should be around 410 °C [22]. However there were problems with composition stability. Our samples, when checked by EDX in the TEM, were low in copper. Some samples had lost almost all of their copper while other samples had nearly fifty percent copper as expected. When preparing the same sample again, different compositions were measured. We endeavored to

determine the cause of our radically different copper amounts. When our samples were made at UCF, Rutherford Backscattering Spectrometry (RBS) was used to calibrate the sputtering equipment (See section 3.2). Thinking that perhaps something went wrong with the deposition, we asked our collaborators in Florida to take RBS of a wafer that had nanoparticles on it. This was not done before because the signal to noise ratio is not good, they had to take data for 24-48 hours in order to get sufficient signal. The RBS data showed that our wafers had close to 50/50 composition of gold to copper as expected from the process steps. It would then seem likely that something in our sample preparation was causing our problem.

We then turned to our sample preparation techniques. Up until this point our samples had always been made using the tripod polishing technique (See section 3.5.1). We took one of our samples that we already prepared for TEM that had close to 50 percent copper and placed it on the hot-plate for one hour. We also took a different sample that had plenty of copper and placed it in a DI water bath for over an hour. These tests would tell us whether the length of time on the hotplate, or length of time exposed to DI water would alter the amount of copper in the samples. There was significant change in the amount of copper before and after the hotplate. Our original AuCu was on average 18% copper and 78% gold. After an hour on the hot plate the compositions were 74.4% copper and 25.6% gold. This would suggest that the sample was losing gold while on the hotplate, however our initial problem was that our samples were losing copper. The strange part is that there was not much change in particle density or particle size. Our particles were 3.43 nm average diameter before the hotplate and 3.34 nm after, well within percent error. Our number of particles per square nanometer was 0.02 before and 0.019 after. We do not currently have a good explanation for why there is such large differences in composition.

The sample that had been in DI water was damaged and that test was inconclusive.

Another researcher in our group, Jordan Batschi, made it his research project to try many different ways of tripod polishing to determine what is causing this compositional instability [23]. He tried using different waxes to adhere the sample to the tripod polisher, alternate chemicals or leaving out chemicals where possible. He also tried skipping the colloidal silica phase. Please see his senior thesis for details. Overall, his results did not show any obvious fixes based on polishing changes.

Supposing the compositional changes were due to our tripod polishing techniques, one sample was made using a FIB technique. See section 3.5.2 for the method. We prepared an unannealed AuCu 5-7 specimen. The sample was prepared by the FIB technique, using a titanium grid. The sample had 37.27% copper close to the TEM grid attachment point and 51.46% copper farther from the grid. The RBS said that this composition should have been 48% copper. This means the percent copper farther from the grid is within our error bars, and is one more reason to believe that something in the tripod polish technique is impacting copper content. The FIB method of sample preparation is frequently used in the semiconductor industry with experienced operators. We do not use it as often in our group because of the amount of time required. For our needs it took a total of about 7 hours spread over two sessions. This is a very long time for just one sample as compared to the tripod polish technique which takes about an hour and a half.

It would appear that copper loss is due to interaction of the exposed particles to the various environments of the polishing process. If so, a possible way to prevent copper losses is to cap the sample with an isolation layer. Addition of a capping layer may limit copper loss and prevent particle growth. However, it also may interfere or interact with our nanoparticles.

4.3.1 Carbon Capping

The first film used was carbon. This is because carbon is inexpensive, and in our research group, there are already a few machines that can deposit carbon. In addition many in our research group have experience with using carbon and depositing carbon. The techniques described in section 3.3.1 were used to coat with carbon. AuCu samples that were made in 2010 were used because there was a large quantity of sample material.

First the carbon coating was done on samples that were on salt substrate. This was done because it makes sample preparation very easy, see Section 3.5.3. Major difficulties were encountered with carbon coatings. The carbon film on salt substrates did not survive the annealing process very well. For many of the attempts when the salt was dissolved there was no film to be seen. In fact, we were not even able to make a single salt substrate sample that had been annealed with carbon. While one possible thought was the carbon and salt were interacting during the anneal, we feel it more likely that the gasses used during the anneals were not sufficiently pure. Argon gas of 99.997% purity was used. The remaining 0.003% is made up of water vapor, and oxygen, both of which can react with and etch carbon during a high temperature anneal. As the films are on the order of 30 nm, it would not take much to etch the film away during the anneal times. Further work would need to be done to determine the exact cause.

Only one unannealed salt substrate sample with carbon on it was successfully made. Our carbon film could be seen on the TEM grid, however, no particles were embedded in the carbon.

Considering there might be a problem with the salt substrate, an unannealed sample on a silicon wafer was coated with carbon. It was annealed in a vacuum system to remove the possibility of gas eating away the carbon layer. However no particles were seen in the TEM for this sample either. One possible cause is that the carbon film might not prevent whatever is in

our tripod polish process from getting to the particles and removing them. The only things that were seen were strange blobs that didn't seem like particles. Due to these many difficulties results are inconclusive as to whether the carbon capping worked.

4.3.2 Alumina Capping

An unannealed AuCu sample was coated with alumina using the techniques of section 3.3.2. This sample was cleaved into several parts for further processing. One alumina capped piece was directly prepared for TEM observation. An anneal at 350 °C for 30 minutes was done on a second piece of the coated specimen. The following questions needed answering; does alumina prevent copper loss, particle growth, and not react with our substrate or particles? See Figure 4-5 for images of the alumina coated samples. In the image on the left you can see holes or thinner spots in the alumina, the annealed sample does not seem to have these holes. We are unsure of the cause of the holes and further work would need to be done to answer this question.

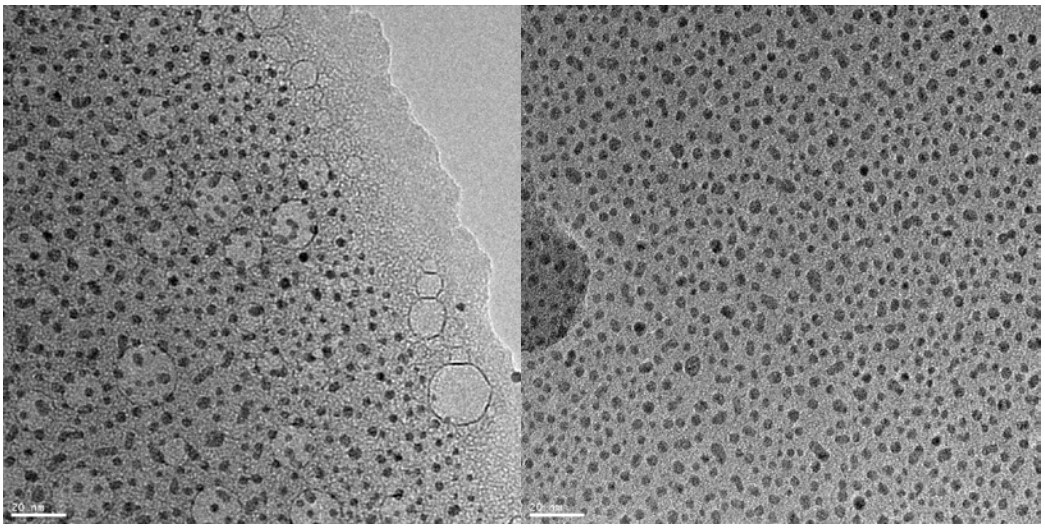

Figure 4-5 Alumina Coated: Unannealed (left) and Annealed (right)

Alumina was found to prevent copper loss. Without capping with alumina our unannealed samples were on average 30.45% copper and 69.55% gold with wide variation between sample locations. Some areas of the sample were as low as 15% copper and other areas were as high as 53% copper. When the samples were capped with alumina the average composition was 51% copper and 49% gold with fluctuations within the technique error estimates. The copper variation from place to place was as low as 49.50% and as high as 52.12%. Alumina capping appears to prevent copper losses during the tripod polishing process and results in absolute compositions as expected from the preparation process.

It is unclear whether alumina can prevent particle growth. Our particles that were unannealed and capped with alumina were on average 3.16 nm in diameter. Our samples that were capped with alumina and then annealed were on average 4.016 nm in diameter. However our samples that were never capped with alumina had average diameters of 3.83 nm and 3.24 nm for the unannealed and annealed respectively. This series was chosen to cap with alumina not because a lot of particle growth was seen, but because there was a lot of this sample available. Since the particle sizes of all four types are sufficiently similar with respect to the observed variations, it is unclear if the alumina prevents particle growth during anneals for these AuCu samples.

It was found that alumina prevented copper losses. Our sample that was annealed with an alumina capping layer had on average 49.34% copper. And our sample that was unannealed and capped with alumina had on average 51% copper and 49% gold. The amount of difference here is certainly small and definitely within our error bars. We can conclude that the alumina prevented copper losses during polishing.

Chapter 5

Conclusion

This project began with the intention of experimentally determining the size effect on the order-disorder temperature of nanoparticles with the hope of directly observing the disordering process as temperature was increased. During the project many difficulties were encountered that prevented the primary study. The greatest was the difficulty in creating ordered particles. Achieving control of particle composition and finding appropriate annealing conditions proved more difficult than anticipated. After many experiments, a set of methods to address these difficulties was determined. This manuscript discusses some of these methods and results.

5.1 FeNiPt

Through Figure 4-4 we were able to show how particle size affects the T_{od}. This was not the direct observation in-situ study we were hoping for, however we still have experimental data showing the effect. When the particles were around 6 nm in diameter there was a shift downward of the T_{od} of 10-15 percent compared to the bulk. While particles around 10 nm in diameter experienced a downward shift of 0-6 percent compared to the bulk. From our data one can approximate that particles less than 10-15nm in diameter would show significant decreases in order-disorder temperature. Remember this is an amount of lowering based only on the size of the particle. These percentages are compared to the T_{od} for that particular compositions bulk value. This method of data analysis is unique and provides a quantitative grasp on the particle size dependence of the order-disorder temperature.

5.2 Alumina Capping

The second major advance achieved by this work is confirming that alumina prevents copper losses during TEM sample preparation. We have shown that when there is no capping layer the copper composition varies greatly from sample to sample and from location to location on the same sample. If however an alumina capping layer is used, the particle composition is as expected and is well within percent error. In addition we showed that when the alumina used is thin enough the images are not adversely affected and charging is not an issue.

Chapter 6

Bibliography

[1] "Material Science," http://nuclearpowertraining.tpub.com/h1017v1/css/h1017v1_25.htm (Accessed April 10, 2013).

[2] H. Numakura* and T. Ichitsubo, "On the stability of chemical order in small ordered-alloy particles," Philosophical Magazine 85, 855–865 (2005).

[3] B. Yang, M. Asta, O. Mryasov, T. Klemmer, and R. Chantrell, "The nature of A1- $L1_0$ ordering transitions in alloy nanoparticles: A Monte Carlo study," Acta materialia 54, 4201–4211 (2006).

[4] G.Wilde, "Nanostructures and nanocrystalline composite materials-synthesis, stability and phase transformations," Surface and interface analysis 38, 1047–1062 (2006).

[5] R. Chepulskii and W. Butler, "Temperature and particle-size dependence of the equilibrium order parameter of FePt alloys," Physical Review B 72, 134205 (2005).

[6] M. Müller, P. Erhart, and K. Albe, "Thermodynamics of $L1_0$ ordering in FePt nanoparticles studied by Monte Carlo simulations based on an analytic bond-order potential," Physical Review B 76, 155412 (2007).

[7] C. Leroux, M. Cadeville, V. Pierron-Bohnes, G. Inden, and F. Hinz, "Comparative investigation of structural and transport properties of $L1_0$ NiPt and CoPt phases; the role of magnetism," Journal of Physics F: Metal Physics 18, 2033 (1988).

[8] F.L. Castillo Alvarado, A. Sukiennicki, c, L. Wojtczak, I. Zasada, "Order–disorder phenomena in binary alloy thin films," Physica B: Condensed Matter. Vol. 344, Issues 1-4, 15 Feb 2004, Pgs 477-488.

[9] "Nanoparticle," http://en.wikipedia.org/wiki/Nanoparticle (Accessed April 12, 2013).

[10] P. Nash, M. F. Singleton, "Phase Diagrams of Binary Nickel Alloys," Vol. 6 (ASM International, 1991), pp. 261-264.

[11] T. Massalski, "Binary Alloy Phase Diagrams," 2nd ed. (Metals Information Society, Metals Park, OH, 1990).

[12] M. Kanellos, “A Divide Over the Future of Hard Drives,” http://news.cnet.com/A-divide-over-the-future-of-hard-drives/2100-1008_3-6108687.html (August 23, 2006)

[13] J.U. Thiele, K. R. Coffey, M. F. Toney, J. A. Hedstrom, A. J. Kellock, “Temperature dependent magnetic properties of highly chemically ordered Fe55ÀxNixPt45L10 films,” Journal of Applied Physics. 91, 6595 (2002).

[14] H. A. Moreen, R. Taggart, D. H. Polonis, “Ni8 X phases in the systems Ni-V, Ni-V-Nb, and Ni-V-Ta,” Journal of Materials Science. Vol 6, Issue 12, Dec 1971, Pgs 1425-1432.

[15] J.T.T. Kumaran, C. Bansal, “Dependence of Average Hyperfine Fields and Order-Disorder Kinetics on Near Neighbour Environments in $Fe_{1-x}Mn_xSi$ Alloys,” Solid State Communications. Vol 74, Issue 10, 1990, Pgs 1125-1130.

[16] K. Ishikawa, H. Mitsui, I. Ohnuma, R. Kainuma, K. Aoki, K. Ishida, “Ordering and phase separation of BCC aluminides in (Ni, Co)–Al–Ti system,” Materials Science and Engineering: A. Vol 329-331, Jun 2002, Pgs 276-281.

[17] R. Kainuma, K. Urushiyama, K. Ishikawa, C.C. Jia, I. Ohnuma, K. Ishida, “Ordering and phase separation in b.c.c. aluminides of the Ni–Fe–Al–Ti system,” Materials Science and Engineering: A. Vol 239-240, Dec 1997, Pgs 235-244.

[18] B. Yao, R. V. Petrova, R. R. Vanfleet, K. R. Coffey, “Compositional stability of FePt nanoparticles on SiO2/Si during annealing,” Journal of Applied Physics. 99, 08E913 (2006).

[19] W. Ostwald, “Textbook of General Chemistry,” 1896, Vol 2, Part 1. Leipzig, Germany.

[20] D.B. Williams, C.B. Carter, “Transmission Electron Microscopy: A Textbook for Materials Science,” 1996, New York: Plenum Press.

[21] A. Jackson, “Experimental Determination of the Pt K Edge K-Factor for Nanoparticle Order-Disorder Transition Analysis,” Senior Honors Thesis (Brigham Young Univeristy, Provo, U.T., 2012, Advisor: Richard Vanfleet).

[22] R. Hultgren, R. D. Desai, D. T. Hawkins, H. G. Gleiser, and K. K. Kelley, “Selected Values of the Thermodynamic Properties of Binary Alloys,” (American Society for Metals, Cleveland, 1973).

[23] J. Batschi, “TEM Sample Preparation for Order-Disorder Temperature Analysis of Au-Cu Nanoparticles,” Senior Thesis (Brigham Young Univeristy, Provo, U.T., 2014, Advisor: Richard Vanfleet).